Temperature-based Model-Predictive Cascade Mitigation in Electric Power Systems

Mads Almassalkhi, *Student Member, IEEE* Ian Hiskens, *Fellow, IEEE*

***Abstract*— This paper proposes a novel model-predictive control scheme which combines both economic and security objectives to mitigate the effects of severe disturbances in electrical power systems. A linear convex relaxation of the AC power flow is employed to model transmission line losses and conductor temperatures. Then, a receding-horizon model predictive control (MPC) strategy is developed to alleviate line temperature overloads and prevent the propagation of outages. The MPC strategy seeks to alleviate temperature overloads by rescheduling generation, energy storage and other network elements, subject to ramp-rate limits and network limitations. The MPC strategy is illustrated with simulations of the IEEE RTS-96 network augmented with energy storage and renewable generation.**

I. Introduction

Recent large-scale electricity supply failures suggest that the power grid is being operated closer and closer to its limits. Without significant capital investment and operational changes, it will not be able to meet future demand [1]. However, as the amount, type and distribution of controllable resources increases, operators will find it increasingly difficult to determine appropriate responses to unanticipated events. For example, energy storage facilities connected to the grid will require consideration of the temporal characteristics of energy control resources. At a minimum, operators will require new tools to guide their decision-making. Given the increased complexity of response actions, a closed-loop feedback process will become indispensable. Furthermore, since power systems are suffused with constraints and limits on states and inputs, model predictive control (MPC) schemes can be particularly useful within the context of contingency management. For an overview of MPC, see [2].

The first application of MPC to emergency control of power systems is [3], where voltage stability was achieved through optimal coordination of load shedding, capacitor switching, and tap-changer operation. A tree-based search method was employed to obtain optimal control actions from discrete switching events. To circumvent tree-based search methods, the authors in [4], [5] employed trajectory sensitivities to develop MPC for voltage stability. However, these methods focus on voltage stability and do not take into account energy storage (ES) or thermal overloads of transmission lines.

Recent literature, see [6], [7], focuses on model-predictive control of electrical systems to alleviate line overloads within a standard DC power flow framework. Specifically, the authors in [7] extend the ideas of [6] to include a linearized current-based thermodynamic model of conductors, which enables [7] to set a hard upper limit on conductor temperature to prevent overloads. An auto-regressive model of the weather conditions (i.e. wind speed and ambient temperature) near transmission lines allows the controller to utilize dynamic ratings and operate the system closer to actual physical limits than if using standard conservative thermal ratings. However, the role of ES in improving economical and secure performance of the system is not considered.

In our previous work [8], a bilevel control scheme was employed for large-scale energy-hub systems. The first level operated on an hour-by-hour timescale with a 24-hour prediction horizon and was in charge of economic dispatch. The second level represented contingency management and was implemented as a simple shrinking (fixed-point) horizon model-predictive cascade-mitigation scheme, which shed minimal load in the process of halting the cascade. The effectiveness of the cascade mitigation process in maximizing economic and secure operation was due to proper management of available ES and renewable energy resources. The impact of different ES scenarios on cascade mitigation was investigated in [9], where it was concluded that the MPC scheme alone provided considerable protection against cascade failures and that appropriate storage schemes further improved performance.

This paper builds upon the model-predictive cascade mitigation scheme presented in [8] by implementing a receding-horizon MPC scheme[1]. The MPC recommendations are implemented with AC power flow measurements and explicitly consider economic set-points (for generation and ES), yet achieves security by bringing line temperature below limits. That is, the MPC scheme drives the system to a secure *and* economical operating region. In addition, an improvement over standard linearization techniques for branch currents is provided in terms of a piece-wise linear convex relaxation that is proven sufficient to alleviate line temperature overloads and mitigate the effects of cascading failures in power systems.

Section II provides an overview of the interaction and roles of Level 1 and Level 2 operations. The Level 2 controller model, including the convex relaxation of line losses is developed in Section III. The model of the actual power system (i.e. the plant) is discussed in Section IV. In Section V, the MPC cascade mitigation scheme is simulated

This work was supported by U.S. Department of Energy under research grant DE-SC0002283 and by ARPA-E under research grant DE-AR0000232.

M. Almassalkhi and and I. Hiskens is with Department of Electrical Engineering: Systems, University of Michigan, 1301 Beal Avenue Ann Arbor, MI 48109, U.S.A. {malmassa, hiskens}@umich.edu

[1]This contrasts with the fixed horizon MPC scheme of [8].

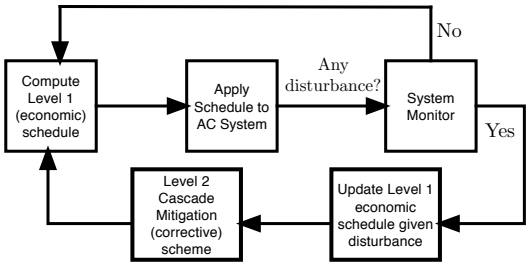

Fig. 1: Overview of proposed control scheme showing Level 1 (economical) and Level 2 (corrective) interaction.

on the IEEE RTS-96 network. Finally, Section VI concludes the paper and suggests future research directions. Due to space constraints, some of the technical details in this paper are omitted. Please see [10] for the missing details.

II. System Operation and Control

The economic dispatch problem allows computation of an economically optimal trajectory, which the system operator tracks via available generation and forecasted load. However, if a significant disturbance takes place, the operator must modify his economical trajectory to prevent overloads and subsequent line outages. This requires the formulation of an emergency (safety) contingency controller, which responds quickly to a disturbance and drives the system back to a secure and economical state, from which economic dispatch can be re-initiated and normal (economic) operation can resume. Therefore, a bilevel hierarchical control strategy is employed for electric power systems.

The "Level 1" controller is enlisted to compute an economically optimal schedule for each hour of the day. When a disturbance takes place (e.g. line outage), Level 1 computes an updated economic reference for the "Level 2" contingency controller, which is initiated and shifts operation from economically optimal (hourly) to corrective (minute-by-minute) in order to alleviate transmission line temperature overloads. Figure 1 gives an overview of the proposed bilevel hierarchical operation of the system, and discussion of each level is included below.

A. Level 1: Optimal Energy Schedule

Over a 24-hour period, an optimal energy schedule determines how to best operate ES, conventional generation, flexible loads, and available renewable energy based on forecasts. The Level 1 schedule is similar to standard economic dispatch [11] but considers grid storage, renewable generation, and line losses. The line losses are modeled with a standard piece-wise linear (PWL) approximation as proposed in [12], [13].

In Level 1, line flow (i.e. thermal) limits are enforced to ensure that, under accurate model and forecast scenarios, no lines are overloaded. The dispatch schedule is computed as a multi-period quadratic programming (QP) problem whose objective is to minimize energy costs of conventional generators:

$$\text{Cost}\,(f_{Gn}) = \alpha_{Gn} f_{Gn}^2 + \beta_{Gn} f_{Gn}, \tag{1}$$

where α_{Gn} [\$/h/pu^2] and β_{Gn} [\$/h/pu] are constant generator-specific parameters and f_{Gn} [pu] is the output power provided by generator n. The only dynamics considered for Level 1 are ES dynamics and ramp-rate limits on generators. Thus, the Level 1 schedule represents a reference signal with economically optimal system set-points, x^{sp}, and the operator control actions u^{sp} required to achieve those set-points. The schedule is submitted to the operator and recomputed every hour. For details on Level 1 formulation, see [8], [14].

B. Level 2: Corrective Control

This lower level generally operates in the background to track the reference trajectories computed from Level 1 (i.e. the economic set-point values). The corrective controller employs a simple linear model of the actual system (i.e. plant), which is described in detail in Section III, and operates on a minute-by-minute timescale. If a disturbance takes place (e.g. line outage), Level 2 computes corrective control actions in a receding-horizon (i.e. moving horizon) MPC fashion that steers the system towards a safe and economically optimal state as provided by a Level 1 post-disturbance schedule update. The MPC scheme can be summarized as follows:

1) At time k and for the measured system state x_k^{meas} and updated reference signals from Level 1, $x^{\text{sp}}[k]$ and $u^{\text{sp}}[k]$, solve an optimal control problem over fixed interval $[k, k+M]$ taking into account the current and future constraints. This yields a sequence of optimal open-loop controls: $\{u[0|k], u[1|k], \ldots, u[M-1|k]\}$ (i.e. $[l|k] \rightarrow$ time $k+l$).
2) Apply first instance of open-loop sequence: $u[0|k]$.
3) Measure the state reached at time $k+1$, x_{k+1}^{meas}.
4) Set $k = k+1$ and repeat step 1).

The time-scale of Level 2 is on the order of minutes to capture the dynamics associated with the temperature of transmission line conductors. At this time-scale, one must consider ramp-rate limits on conventional generators, dynamics and power ratings of grid storage devices, and incorporate the thermal response of overloaded lines. Note that in Level 2, lines are no longer subject to a hard flow limit constraint and, instead, the controller seeks to drive line temperatures below their respective limits and return generation and storage to economical set-points.

III. Controller Model

The Level 2 MPC controller utilizes a simplified but sufficient approximate model of the non-convex AC power system that is amenable to a linear optimization framework. The index l denotes discrete time-steps of one minute and the MPC scheme is employed with prediction and control horizon M. For notational convenience, the time index $[l|k]$ is replaced with l.

An electric power system network can be described in a graph-theoretic sense as consisting of a set of nodes and edges, (i.e. edge $(i,j) \in \mathcal{E}$ for nodes $i,j \in \mathcal{N}$, graph $\mathcal{G} = (\mathcal{E},\mathcal{N})$). Electrical transmission lines have prescribed power flow limits to prevent dangerous sagging and permanent damage (e.g. annealing). These limits are related to the thermal capacity of the conductor and the current flowing across the line. Generally, there is an inverse relationship between the current on a line and the expected time it takes before the line must be taken out of service. In most common overload scenarios, the time-response is of the order of 10-20 minutes [15]. To ensure secure line flows, it is desirable for an operator to enforce flows to stay within apparent power (MVA) limits. While it is feasible to take such limits into consideration upon determination of an hourly energy management schedule (i.e. Level 1), it is unrealistic to expect such a constraint to be valid immediately after a significant disturbance (e.g. line outage). This is because flows depend on the physics of the network and (unlike many digital systems) cannot be directly guided, which means that line flows may exceed their limits post-contingency. Therefore, in Level 2, line overloads are tracked via the conductor temperature and the controller seeks to alleviate temperature overloads.

The states and inputs associated with the proposed formulation of a MPC cascade mitigation scheme for an electric power system are outlined below.

Dynamic states: there are three types of dynamic states:

- $\Delta\hat{T}_{ij}$, line (i,j) conductor temperature overload with respect to limit, T_{ij}^{lim}.
- E_n, state-of-charge (SOC) for ES n
- f_{Gn}, power output level for generator n.

Control inputs: the formulation employs six types of control inputs:

- Δf_{Gn}, change to conventional generator n output level
- $f_{G_W n}^{\text{spill}}$, wind spilled from nominal wind turbine n
- f_{Dn}^{red}, load reduction from nominal load n
- $f_{Q\text{c},n}$, $f_{Q\text{d},n}$, charge (c), discharge (d) rates for ES n
- ψ_{ij}, transformer phase shift (rads) for line (i,j).

Uncontrollable inputs: there are three types of forecasted (uncontrollable) inputs (i.e. disturbances):

- $f_{G_W n}^{\text{nom}}$, nominal available power from wind turbine n
- f_{Dn}^{nom}, nominal demand for load n
- d_{ij}, ambient temperature and solar gain for line (i,j).

Algebraic states: consider six types of algebraic states:

- f_{ij}, real power flowing across line (i,j)
- f_{ij}^{loss}, real power loss from line (i,j)
- θ_{ij}, phase angle difference between nodes i and j
- $f_{G_W n}$, real power injected from wind turbine n.
- f_{Dn}, real power consumed by load n.
- f_{Qn}, total power injected or consumed by ES n.

Suppose that controls $u(t)$ are step-wise with step-width T_s [s], such that $u(t) := u[k]$ for $t \in [kT_s, (k+1)T_s]$. All discrete dynamics are the result of forward Euler discretization with sample time T_s. For each time k, the dynamic states x_k^{meas} are measured perfectly and represent the initial state of the MPC system model. Then, the full MPC formulation is defined as a quadratic programming (QP) problem:

$$\min_{u[l]} \quad \left|\left|x[M] - x_{k+M}^{\text{sp}}\right|\right|_{S_M} + \sum_{l=0}^{M-1} L\left(x[l], u[l]\right) \tag{2a}$$

s.t.

$$\Delta T_{ij}[l+1] = \tau_{ij}\Delta T_{ij}[l] + \rho_{ij}\Delta f_{ij}^{\text{loss}}[l] + \delta_{ij}\Delta d_{ij} \tag{2b}$$

$$E_n[l+1] = E_n[l] + T_s\eta_{\text{c},n} f_{Q\text{c},n}[l] + \frac{T_s}{\eta_{\text{d},n}} f_{Q\text{d},n}[l] \tag{2c}$$

$$f_{Gn}[l+1] = f_{Gn}[l] + \Delta f_{Gn}[l] \tag{2d}$$

$$0 = \Gamma_i\left(f_{ij}[l], f_{ij,k}^{\text{loss,est}}, f_{Gn}[l], f_{Dn}[l], f_{Q,n}[l]\right) \tag{2e}$$

$$0 = a_{ij}x_{ij}f_{ij}[l] - \left(\theta_{ij}[l] - \psi_{ij}[l]\right) \tag{2f}$$

$$0 = a_{ij}x_{ij}^2 f_{ij}^{\text{loss}}[l] - r_{ij}\left(\theta_{ij}[l] - \psi_{ij}[l]\right)^2 \tag{2g}$$

$$\Delta\hat{T}_{ij}[l] = \max\{\Delta T_{ij}[l], 0\} \tag{2h}$$

$$f_{Dn}[l] = f_{Dn}^{\text{nom}}[l] - f_{Dn}^{\text{red}}[l] \tag{2i}$$

$$f_{Q,n}[l] = f_{Q\text{c},n}[l] + f_{Q\text{d},n}[l] \tag{2j}$$

$$f_{G_W n}[l] = f_{G_W n}^{\text{nom}}[l] - f_{G_W n}^{\text{spill}}[l] \tag{2k}$$

$$x[l] \in \mathcal{X},\ u[l] \in \mathcal{U},\ z[l] \in \mathcal{Z} \tag{2l}$$

$$x[M] \in \mathcal{T}_x \tag{2m}$$

$$x[0] = x_k^{\text{meas}} \tag{2n}$$

for all $l \in \mathcal{M}$, where $x[l]$, $u[l]$, and $z[l]$ represent the dynamic state, control input, and algebraic state variables, respectively, at predicted time $k+l$ given initial measured state at time k, x_k^{meas}. The terms in the summation of the objective function (2a) are defined by:

$$L(x[l], u[l]) = ||x[l] - x_{k+l}^{\text{sp}}||_Q + ||u[l] - u_{k+l}^{\text{sp}}||_R, \tag{3}$$

where $||y||_B \equiv y^\top By$ and $S_M \succeq 0$, $Q \succeq 0$, $R \succeq 0$ are positive semi-definite weighting matrices.

Expressions (2b), (2c), and (2d) represent the linear (discrete) dynamics associated with conductor temperature for line (i,j), SOC for energy storage device n, and the output level of generator n, respectively. The thermal conductor model is based on the IEEE standard describing the temperature-current relationship in overhead conductors [16]. Temperature dynamics in (2b) are linearized with respect to the conductor temperature (T_{ij}^{lim} [°C]) at ampacity (I_{ij}^{lim} [A]), and conservative ambient parameters. That is, $\Delta T_{ij} = T_{ij} - T_{ij}^{\text{lim}}$ and $\Delta f_{ij}^{\text{loss}} = f_{ij}^{\text{loss}} S_b/3L_{ij} - R_{ij}(I_{ij}^{\text{lim}})^2$, where S_b [VA/pu] and L_{ij} [m] are power base and conductor length, respectively, and R_{ij} [Ω/m] is the per-unit length resistance.

Equations (2e), (2f), and (2g) denote nodal power balance constraints ($\forall i \in \mathcal{N}$), DC power flows, and nonlinear DC-based active line losses, respectively. The scalar values x_{ij} and r_{ij} are the per-unit (pu) line reactance and resistance. Power balance implies Kirchhoff's 2nd law: that power flowing into node i must equal the power flowing out of the node i plus/minus what is injected/consumed at node i, and is defined as follows:

$$0 = \sum_{j \in \Omega_i^{\text{N}}} f_{ij}^{\text{T}}[l] - \sum_{n \in \Omega_i^{\text{G}}} f_{\text{G}n}[l] + \sum_{n \in \Omega_n^{\text{E}}} f_{Qn}[l] + \sum_{n \in \Omega_D^{\text{D}}} f_{\text{D}n}[l] \tag{4}$$

where $f_{ij}^{\mathrm{T}} := f_{ij} + \frac{1}{2} f_{ij}^{\mathrm{loss}}$ is the total flow on line (i,j) with

- Ω_i^{G}, set of generators (conventional & wind) at node i
- Ω_i^{N}, set of adjacent nodes to node i
- Ω_i^{D}, set of demands at node i
- Ω_i^{E}, set of energy storage devices at node i.

Note that DC flow and losses, as presented in (2f) and (2g), reflect application of the "Unified Branch Model" as developed by [17]. Under the unified model, in-phase (IPT, $\psi_{ij} = 0$) and phase-shifting (PST, $a_{ij} = 1$) transformers and transmission branches ($a_{ij} = 1$, $\psi_{ij} = 0$) can be described together.

Constraint (2h) defines the main objective of alleviating temperature overloads while not incentivizing underloading of lines. That is, the MPC should compute control actions that only take into account lines with $\Delta T_{ij}[l] > 0$. Keeping in mind the QP formulation, the temperature objectives of MPC are defined as follows:

$$\Delta \hat{T}_{ij} = \max\{0,\, \Delta T_{ij}\} \Longrightarrow \left\{ \begin{array}{c} 0 \le \Delta \hat{T}_{ij} \\ \Delta T_{ij} \le \Delta \hat{T}_{ij} \end{array} \right. . \quad (5)$$

Algebraic equations (2i), (2j), (2k) define the relationship between control inputs and power balance from (2e). Specifically, how load shedding, injections/consumption by storage, and wind curtailment are coupled with generation and line flows within the electric network.

The sets defined in (2l) and (2m) are all convex polytypes. In particular, $\mathcal{X} \ni x_{\mathrm{sp}}$ is closed and $\mathcal{U} \ni u_{\mathrm{sp}}$ is compact:

$$\mathcal{X} = \left\{ \mathbf{x} \,\middle|\, E[l] \in [0, \overline{E}]; f_G[l] \in [\underline{f_G}, \overline{f_G}]; \Delta \hat{T}[l] \ge 0 \right\} \quad (6)$$

$$\mathcal{Z} = \{ \mathbf{z} \,|\, \theta_{ij}[l] \in [-\theta^{\max}, \theta^{\max}] \subset (-\pi/2, \pi/2) \} \quad (7)$$

$$\mathcal{U} = \Big\{ \mathbf{u} \,\Big|\, f_{\mathrm{D}}^{\mathrm{red}}[l] \in [0, \alpha_{\mathrm{D}}], f_{\mathrm{G_w}}^{\mathrm{spill}}[l] \in [0, \alpha_{\mathrm{G}}], \quad (8)$$
$$\Delta f_{\mathrm{G}}[l] \in [-R_{\mathrm{G}}^{\mathrm{down}}, R_{\mathrm{G}}^{\mathrm{up}}], \psi_{ij}[l] \in [-\alpha_P, \alpha_P],$$
$$f_{Q\mathrm{c}}[l] \in [0, \overline{f}_{Q\mathrm{c}}], f_{Q\mathrm{d}}[l] \in [-\overline{f}_{Q\mathrm{d}}, 0] \Big\}$$

with bounds defined by appropriate parameters.

Finally, the set $\mathcal{T}_x \subset \mathcal{X}$ establishes a convex polytopic terminal constraint set that forces all line temperatures to be at or below their limits by the end of the prediction horizon. The terminal set is defined as follows:

$$\mathcal{T}_x = \left\{ \mathbf{x} \,\middle|\, \Delta \hat{T}[M] = 0; E[M] \in [0, \overline{E}]; f_G[M] \in [\underline{f_G}, \overline{f_G}] \right\} \quad (9)$$

The astute reader will have noticed the nonlinear and non-convex description of active line losses in (2g). In the next section, a convex relaxation of line losses is developed and proven to be tight for overloaded lines.

A. Convex Relaxation of Line Losses

To include a meaningful model of losses into the QP formulation, a PWL relaxation of losses that circumvents the need for integer optimization is applied, similar to [12], [13]. To simplify notation in the development of the PWL approximation, let transformer parameters $a_{ij} = 1$ and $\psi_{ij} = 0$.

The DC loss formulation in (2g) will be approximated using S linear segments of width $\Delta\theta$. Denote the slopes of each segment $\alpha_{ij}(s)$ and define variables $\theta_{ij}^{\mathrm{PW}}(s)$, $\forall s \in \{1, \ldots, S\}$, such that:

$$f_{ij}^{\mathrm{loss}} \approx \mathrm{PWL}\left[\frac{r_{ij}}{x_{ij}^2} \theta_{ij}^2 \right] = \sum_{s=1}^{S} \alpha_{ij}(s) \theta_{ij}^{\mathrm{PW}}(s), \quad (10)$$

where PWL[.] is a piece-wise linear approximation. Implementation of PWL[.] within an optimization framework generally requires binary integers to enforce adjacency conditions for PWL segments [18]. Adjacency conditions ensure that $\theta_{ij}^{\mathrm{PW}}(s) > 0 \Rightarrow \theta_{ij}^{\mathrm{PW}}(p) = \Delta\theta$, $\forall p < s$. On the contrary, if one omits integers and relaxes adjacency conditions, it implies a strictly continuous LP approximation of line losses that is equivalent to a bounded convex relaxation of PWL[.]. The linear relaxation is convex since segment slopes are monotonically increasing for all l (when $r_{ij} > 0$):

$$(2s-1)\frac{r_{ij}}{x_{ij}^2}\Delta\theta = \alpha_{ij}(s) < \alpha_{ij}(s+1) = 2s\frac{r_{ij}}{x_{ij}^2}\Delta\theta. \quad (11)$$

The PWL approximation is a relaxation when adjacency conditions are not enforced, as illustrated in Figure 2a and by the following:

$$f_{ij}^{\mathrm{loss}} \approx \mathrm{PWL}[f_{ij}^{\mathrm{loss}}] \le \sum_{s=1}^{S} \alpha_{ij}(s) \theta_{ij}^{\mathrm{PW}}(s) \quad (12)$$

$$= \frac{r_{ij}}{x_{ij}^2} \Delta\theta \sum_{s=1}^{S} (2s-1) \theta_{ij}^{\mathrm{PW}}(s), \quad (13)$$

where variables $\theta_{ij}^{\mathrm{PW}}(s)$ are defined by

$$|\theta_{ij}| = \sum_{s=1}^{S} \theta_{ij}^{\mathrm{PW}}(s) \quad (14)$$

with $\theta_{ij}^{\mathrm{PW}}(s) \in [0, \Delta\theta_{ij}]$ providing the contribution to $|\theta_{ij}|$ for each segment $s = 1, ..., S$ of the PWL approximation. To model the (non-convex) absolute value relation in (14) within an LP formulation, apply the following relaxation:

$$\theta_{ij} = \theta_{ij}^{+} - \theta_{ij}^{-}, \qquad \sum_{s=1}^{S} \theta_{ij}^{\mathrm{PW}}(s) := \theta_{ij}^{+} + \theta_{ij}^{-} \quad (15)$$

where $\theta_{ij}^{+}, \theta_{ij}^{-} \in [0, \theta^{\max}]$. This is equivalent to a bounded convex relaxation of (14), as demonstrated in Figure 2b and below:

$$|\theta_{ij}| = |\theta_{ij}^{+} - \theta_{ij}^{-}| \le |\theta_{ij}^{+}| + |\theta_{ij}^{-}| = \theta_{ij}^{+} + \theta_{ij}^{-}. \quad (16)$$

Notice that in the absence of enforcing the complementarity condition: $\theta_{ij}^{+}\,\theta_{ij}^{-} = 0$, the convex relaxation may overestimate $|\theta_{ij}|$ and, hence, overestimate losses.

In summary, the convex relaxation of active line losses is described by the algebraic states $\theta_{ij}^{+}, \theta_{ij}^{-}, \{\theta_{ij}^{\mathrm{PW}}(s)\}_{s=1}^{S}$ and

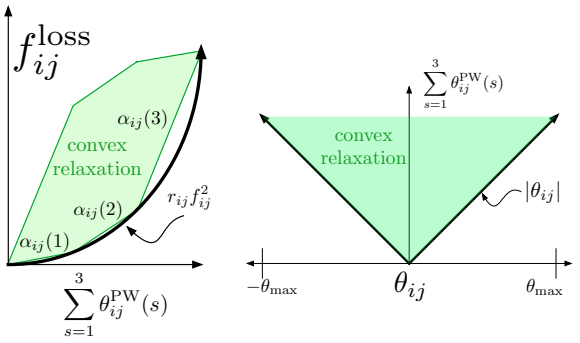

(a) PWL adjacency relaxation (b) Absolute value relaxation

Fig. 2: Relaxing adjacency conditions and absolute value complementarity condition (i.e. $\theta_{ij}^{+}\theta_{ij}^{-}=0$) for PWL approximation with $S=3$. Notice how the PWL segment variables $\theta_{ij}^{\text{PW}}(s)$ define the relationship between phase angles and line losses.

the following expressions, which replace (2g):

$$f_{ij}^{\text{loss}} := \frac{r_{ij}}{a_{ij}x_{ij}^2}\Delta\theta\sum_{s=1}^{S}(2s-1)\theta_{ij}^{\text{PW}}(s) \tag{17a}$$

$$\sum_{s=1}^{S}\theta_{ij}^{\text{PW}}(s) = \theta_{ij}^{+}+\theta_{ij}^{-} \tag{17b}$$

$$\theta_{ij}-\psi_{ij} = \theta_{ij}^{+}-\theta_{ij}^{-} \tag{17c}$$

$$\theta_{ij}^{+},\theta_{ij}^{-}\geq 0 \tag{17d}$$

$$\theta_{ij}-\psi_{ij}\in[-\theta_{\max},\theta_{\max}] \tag{17e}$$

$$\theta_{ij}^{\text{PW}}(s)\in[0,\Delta\theta]. \tag{17f}$$

The linear formulation presented in (17) produces losses that are greater than or equal to PWL$[f_{ij}^{\text{loss}}]$. Equality occurs only when both absolute value complementarity (i.e. $\theta_{ij}^{+}\,\theta_{ij}^{-}=0$) and PWL adjacency conditions are satisfied. Under such conditions, the relaxation is considered "tight" and the model is exact (with respect to PWL$[f_{ij}^{\text{loss}}]$). Furthermore, when the losses are relaxed (i.e. not tight), overestimated losses are denoted "fictitious losses" as they exist only as a figment of the MPC controller model and not in the real system (plant).

To that effect, the MPC scheme must exhibit a tight approximation of line losses when temperatures are above their limit to allow overloaded lines to be driven below their limit. The following theorem describes sufficient conditions that enable a tight approximation.

Theorem III.1 (Temperature & Convex Relaxation) *Assume $r_{ij}>0$ and losses in* (2e) *are fixed to an estimated value over duration of the prediction horizon. If the temperature of line $(i,j)\in\mathcal{A}$ exceeds its limit at time $l+1$, then the convex relaxation is tight with respect to line (i,j) for all previous time-steps. That is, if $\exists l\in\{0,\dots,M-1\}$ and $(i,j)\in\mathcal{A}$ such that $\Delta T_{ij}[l+1]>0$, then adjacency conditions are satisfied and $\theta_{ij}^{+}[p]\theta_{ij}^{-}[p]=0\ \forall p\leq l$, which implies that the convex relaxation associated with line (i,j) is tight for all time $p\leq l$.*

Proof: The full proof is given in [10]. To sketch the proof, let $\{\Delta T_{ij}[l]\}_{l=1}^{M}$ be an optimal MPC temperature trajectory for line (i,j) and assume $\exists l\in\{0,\dots,M-1\}$ such that $\Delta T_{ij}[l+1]>0$ but the solution is **not** tight for some $p\leq l$. That is, losses are overestimated via the convex relaxation (i.e. either $\theta_{ij}^{+}[p]\theta_{ij}^{-}[p]>0$ and/or adjacency conditions are not satisfied in the PWL relaxation, see Figure 2). Then, a feasible solution can be derived which is identical to the optimal solution except that it enforces a tight formulation at time p and reduces line losses accordingly, say from $f_{ij,\text{relax}}^{\text{loss}}[p]>f_{ij,\text{tight}}^{\text{loss}}[p]$. Decreased losses at time p result in lower temperatures from time $p+1$ onwards, which implies that the temperature overload at time $l+1$ must be less under the tight feasible solution. Since the objective function penalizes $\Delta\hat{T}_{ij}[p]$, the feasible tight trajectory embodies a lower cost solution than the relaxed optimal trajectory. This is a contradiction. Thus, if (i,j) has a temperature overload at time $l+1$, the formulation is locally tight $\forall\, p\leq l$. ■

Given the complete controller model description provided by (2), (17), the state and input vectors can be collected together as:

$$x = col\{\Delta\hat{T}, E, f_G\} \tag{18a}$$

$$u = col\{\Delta f_G, f_{G_W}^{\text{spill}}, f_D^{\text{red}}, f_{Q\text{c}}, f_{Q_\text{d}}, \psi\} \tag{18b}$$

$$z = col\{\theta, \theta^{+}, \theta^{-}, \theta^{PW}, f, f^{\text{loss}}, f_D, f_{\text{G}_\text{W}}, f_Q\}. \tag{18c}$$

B. Objective Weighting Matrices

One of the objectives of the MPC scheme is to determine optimal control actions to alleviate temperature overloads, $\Delta\hat{T}_{ij}$. Described below are the multiple objectives that the MPC balances to compute optimal corrective control actions:

$$\begin{aligned}
p_o(\Delta\hat{T}_{ij}[l])^2 &\quad \text{- line temperature overload}\\
p_g(f_{\text{G}n}[l]-f_{\text{G}n}^{\text{sp}})^2 &\quad \text{- deviation from reference output}\\
p_r(\Delta f_{\text{G}n}[l]-\Delta f_{\text{G}n}^{\text{sp}})^2 &\quad \text{- changes in generation ramping}\\
p_e(E_n[l]-E_n^{\text{sp}})^2 &\quad \text{- deviation from reference SOC}\\
p_q(f_{Q\text{d/c}n}[l]-f_{Q\text{d/c}n}^{\text{sp}})^2 &\quad \text{- changes in reference dis/charging}\\
p_s(f_{\text{D}n}^{\text{red}}[l])^2 &\quad \text{- load control}\\
p_w(f_{\text{G}\text{w}n}^{\text{spill}}[l])^2 &\quad \text{- wind spill}\\
p_p(\psi_{ij}[l]-\psi_{ij}^{\text{sp}})^2 &\quad \text{- deviation from PST reference}
\end{aligned}$$

The reference values above, denoted $(.)^{\text{sp}}$, refer to the economically optimal set-points computed in Level 1. To prioritize objectives, the coefficients $p_{(.)}>0$ take on different values. However, the main objective is to drive temperatures below their limits.

Based on the state and input definitions in (18), the weighting matrices in (2a) are given by:

$$Q = diag\{p_oI, \frac{p_e}{10M^2}I, \frac{p_g}{10M^2}I\}\succeq 0 \tag{18d}$$

$$S_M = diag\{p_oI, p_eI, p_gI\}\succeq 0 \tag{18e}$$

$$R = diag\{p_rI, p_wI, p_sI, p_qI, p_qI, p_pI\}\succ 0. \tag{18f}$$

where I represents square identity matrices of appropriate dimensions and $diag\{.\}$ is a block-diagonal matrix. Note

that the terminal cost matrix, S_M, penalizes deviations from economical references for storage SOC and conventional generation states more severely than Q. This is because, the MPC does not care *how* these reference signals are tracked, only that they are being considered by the end of the horizon.

Remark III.2 (From DAE to ODE) *The DAE system presented in* (2) *cannot be written explicitly as an ODE, because there is no bijective mapping from algebraic to dynamic states. That is, the convex relaxations employed in this MPC model beget multiple optimal algebraic solutions for lines that satisfy* $\forall l,\ \Delta\hat{T}_{ij}[l] = 0$.

IV. Plant (Actual) Model

The AC power flow is generally accepted as a valid representation of the actual physical power system. Therefore, the control actions recommended by the MPC scheme, which utilizes the strictly linear model described in Section III, is applied to an AC model of the system at each time-step. In addition, resulting losses from the full AC power flow are utilized in a non-linear temperature model to capture the effects of MPC recommendations on the actual system. Finally, the actual energy storage model does not allow for simultaneous charging and discharging in the same time-step.

Excessive line temperature (and resulting sag or possible annealing) may eventuate in line-tripping. The higher the temperature, the more likely line tripping becomes. To capture the inverse relationship between temperature and expected-time-to-trip in the actual system, the exponential probability distribution function is utilized and the conditional probability of tripping line (i, j), given line temperature at time k, is defined as follows:

$$P\left(\text{line } (i,j) \text{ trips at } k\right) = 1 - e^{-\lambda(\Delta T_{ij}[k])T_s} \tag{19}$$

with rate parameter $\lambda > 0$ determined based on the short-term (15-minute) emergency (STE) rating. The proposed model employs $\lambda(\Delta T_{ij}[k]) = (\Delta T_{ij}[k]/30)^6$.

Furthermore, considering over-current protection on transmission lines (for large overloads), an additional condition is added to the probabilistic line-tripping model:

$$P\left(\text{ line } ij \text{ trips at } k \,\middle|\, |f_{ij}^{\text{ac}}[k]| \geq f_{ij}^{\text{lim}}\overline{\Omega}\right) = 1 \tag{20}$$

where f_{ij}^{ac} [pu] is a line's AC power flow in the actual system and $\overline{\Omega}$ is an upper bound on allowable relative instantaneous overload. For example, if $\overline{\Omega} = 3$, then a line flow of 300% of f_{ij}^{lim} automatically and immediately trips line (i, j).

V. Numerical Example: IEEE RTS-96

This example will highlight the advanced contingency management available from the proposed hierarchical control scheme. The MPC scheme is applied to an augmented version of the IEEE RTS-96 power system test-case, which is described in full details in [19] (i.e. load, generator, transmission, transformer, and bus parameters) and illustrated in Figure 3. However, the RTS-96 system is designed as a highly reliability system with large nominal thermal ratings. To bring the system closer to its limits and engender worthwhile scenarios, thermal ratings have been reduced by 40%, which means that line temperature limits are reduced to the range of 60-70°C. Furthermore, ramp-rates have been reduced by 82.5% to enhance the role of storage in congestion management and highlight Level 2 performance. For more details, please see [10].

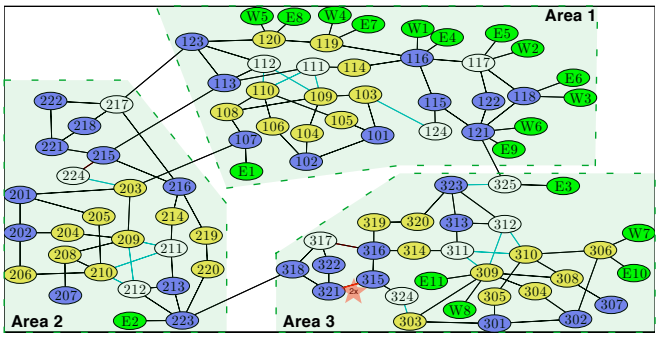

Fig. 3: Augmented IEEE RTS-96 one-line diagram with storage (E) wind (W). Specific buses are denoted with three digits. Bus types are indicated by color: generator (blue), load (yellow), and through-put (white). Edges represent transmission lines (black) and transformers (gray). The disturbance (i.e. tripped lines) is displayed with a star. Storage and wind nodes are attached to buses as indicated, but those edges do not represent transmission lines.

To benchmark the performance of the proposed MPC-based scheme, a base-case controller is employed.

A. Base-case Controller

The base-case controller estimates human control operator behavior during a large disturbance. Modeling a human operator is non-trivial, however, the crude base-case presented here captures the underlying goals of the operator [20], which are implemented within an MPC-based framework:

1) Consider power overloads and not temperature.
2) Employ power transmission distribution factors (PTDFs), generation shift factors (GSFs), and transmission loading relief (TLR) procedures to make control decisions to reduce overloads.
3) Energy storage devices are not available for control.

- **Base-case implementation**
  - Replace $\Delta\hat{T}[l]$ with static power overload: $\hat{o}_{ij}[l] = 10\max\{0, (|f_{ij}[l]| + \frac{1}{2}f_{ij}^{\text{loss,est}}[k])/f_{ij}^{\text{lim}} - 1\}$. That is, if a line is 10% overloaded, $\hat{o}_{ij} = 1.0$.
  - Consider PTDFs, GSFs, and TLR procedures implicitly as a 1-step MPC process akin to Level 2 (i.e. set $M = 1$) but include overloads $\hat{o}_{ij}[0|k]$, $\hat{o}_{ij}[1|k]$ in objective and terminal costs.
  - Ignore terminal constraints $\mathcal{T}_x$.
  - Set $R_{\text{base}} = R$, $Q_{\text{base}} = S_M$, $S_{M,\text{base}} = S_M$

The objective weighting factors utilized in MPC Level 2 and base-case are presented in Table I. Note that overload coefficient, p_o, for the base-case, reflects power overload ($\hat{o}_{ij}$) and not temperature. Also, the storage control coefficient for the base-case, $p_q = \infty$, is to reflect that this

TABLE I: Objective function coefficients for Q, R, S_M matrices for MPC and base-case systems.

Model	p_o	p_e	p_g	p_r	p_w	p_s	p_q	p_p
Lvl 2	1	100	100	[0.05,1]	0.05	100	0.1	0.05
Base	5	0.01	0.01	[0.01,0.1]	0.10	200	∞	0.1

resource is not available in decision-making. Control changes to generator inputs, Δf_G, are penalized with factors $p_r = \max\{0.05, \alpha_G / \max_G \{\alpha_G\}\}$ in Level 2 while for the base-case: $p_r = 0.1 \max\{0.1, \alpha_G / \max_G \{\alpha_G\}\}$. Recall, α_G is given by cost-curve (1). The cost-curve parameters (α_G, β_G) utilized in this example are from [21].

Since longer timescales are associated with the early stages of a cascade failure, it allows for significant computation immediately following a disturbance. Therefore, the updated economically optimal set-points are computed by Level 1 immediately following the disturbance.

B. Simulation Results

The RTS-96 model is simulated according to Level 1, Level 2, and base-case implementations. Initially, the system is operated economically according to Level 1. However, at hour 18 when available wind power is low and demand is high, a two-line outage (i.e. disturbance) trips the two parallel lines 315-321. Performance and behavior of Level 2 MPC (with $M = 10, 20, 40$) and the base-case are discussed below.

The two-line outage, at hour 18, causes transmission lines 316-317 and 223-318 to become heavily overloaded. The Level 2 MPC scheme alleviates the temperature overloads and brings the system safely to the updated economic set-points provided by Level 1. However, the base-case cannot relieve the overloads fast enough and undergoes a cascading failure, which evolves as follows:

- $k = 9$: line 316-317 trips with $\Delta T_{ij}[9] = 12.6\,^{\circ}\text{C}$.
- $k = 11$: line 223-318 trips with $\Delta T_{ij}[11] = 16.5\,^{\circ}\text{C}$.
- $k = 12$: Area 3 islands. **Blackout** for small island.
- $k > 12$: Load shed & line overloads. Non-economical.

In the base-case, islanding causes a large long-lasting mismatch between generation and load in the small 4-node island. It is reasonable to conclude that the 4-node island will undergo severe frequency deviations and experience a blackout. Since frequency response is not considered in this study, the large island may overcome its smaller mismatch but, nonetheless, it cannot return to economically optimal operations and sheds up to 12% of total load during 90 minutes.

The actual maximum line temperature overload $\max_{ij}\{\Delta \hat{T}_{ij}[k]\}$ for the base-case and each MPC run is illustrated in Figure 4. Note that MPC is able to avoid high temperature overloads and drive the temperatures below their respective limits by minute $k \approx 40$. After this time, radial line 307-308 hovers 0.6°C above its temperature limit. However, this is due to model inaccuracy regarding the non-linear temperature and AC power system models in the plant and the linear temperature and DC models employed in Level 2 and Level 1. In particular, the temperature

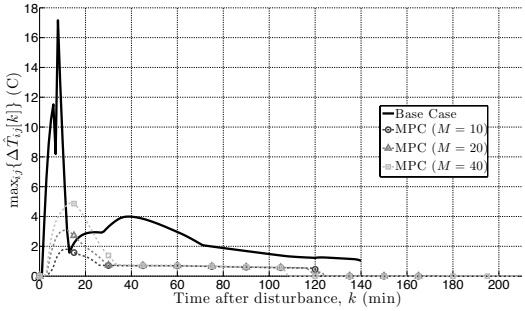

Fig. 4: Maximum line temperature for the base-case and different MPC runs.

deviations above limits are associated with the 138 kV lines that exhibit $x_{ij}/r_{ij} < 4$, which engenders discrepancies in the DC approximation of an AC system. Essentially, the DC model incorrectly informs the controller that losses are low enough that the temperature will drop below its limit in the next time-step under negligible control action. Then, the AC power flow yields higher-than-DC losses and temperature stays above limit. The controller repeats these incorrect estimates until control action is required or load-patterns autonomously reduce line loadings. Power flows associated with the model inaccuracy are, however, less than 5% above $f_{ij}^{\lim}$ for $k > 40$, which is still within expected DC approximation error levels [22].

Comparing the MPC runs to the base-case, a major factor for the improved performance are load and storage control. Namely, by initially shedding no more than 4% of the aggregate load and curtailing reference storage injections, the MPC brings temperatures within limits. For $k > 120$, storage injections in the MPC runs exceed reference levels slightly to bring SOC back to economical reference levels while wind curtailment is employed as cheap control to keep temperatures below limits under model inaccuracy.

The MPC scheme performs a balancing act between economically optimal performance and ensuring safety criteria. This balance is highlighted in Figure 5, where the cost of generation is illustrated for MPC runs and the base-case. To ensure safety, the different MPC cases initially sacrifice economical optimality by deviating from the Level 1 set-points. For $k > 120$, the system returns to economically optimal levels with model inaccuracy causing minor discrepancies.

It is worthwhile to point out the effect on performance from varying the prediction horizon. By employing the terminal constraint $\mathcal{T}_x$, MPC is required to bring temperatures within their limits by the end of the horizon. Therefore, as the prediction horizon decreases, the MPC scheme utilizes more aggressive controls, but the temperature overloads and the departures from economic references (as established by generation costs) are, generally, less severe.

Finally, to illustrate the locally tight convex relaxation from Theorem III.1, Figure 6 presents the adjacency, absolute-value, and temperature conditions for MPC predictions $[l|1]$ (i.e. $l \in \{0, 1, \ldots, M-1\}$ given $k = 1$) with prediction horizon $M = 40$. Notice, how any predicted

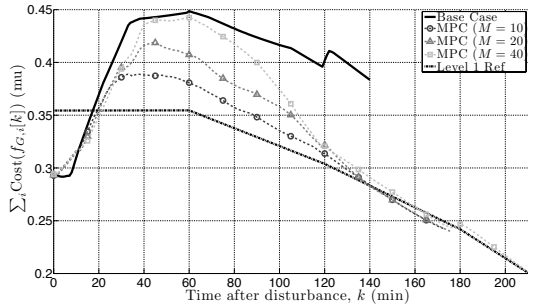

Fig. 5: Economical cost of generation for MPC and Base-case runs with reference provided by Level 1.

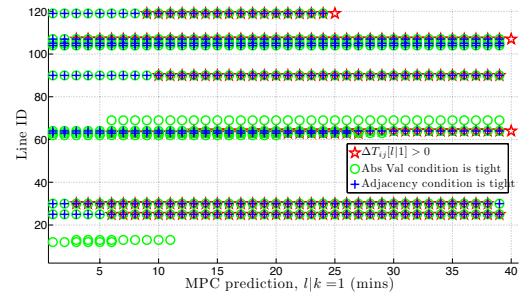

Fig. 6: Illustration that $\Delta T_{ij}[l|k] > 0$ is a sufficient condition for MPC and ensures a locally tight formulation of line losses.

temperature overloads at time $l+1$ yields a tight relaxation for all previous time-steps $p \leq l$. For example, line 119 (223-318) is predicted to have a temperature overload for $l \in [9, 25]$ and adjacency and absolute values relaxations are tight for all $l \leq 24$. This is exactly as stated in the theorem.

VI. Conclusions and Future Work

This paper presents a model predictive control (MPC) approach to managing contingencies in electric power systems. A bilevel hierarchical control scheme is proposed for balancing economic and security objectives. The upper level establishes economic set-points, whilst the lower level exploits the thermal inertia of transmission line conductors to manage post-contingency overloads. The nonlinear relationship between AC power flow and line temperature is captured via a convex relaxation of a PWL formulation for line losses. The MPC scheme is illustrated with an example.

Future work will focus on formally guaranteeing stability of the proposed MPC scheme. In addition, since topological and operational disturbances in large power systems are not generally system-wide, non-centralized schemes will be considered to ensure reasonable computational requirements. This implies a need for adapting control areas based on sensitivities and the nature of the contingencies [23], [24].

VII. Acknowledgements

The authors would like to thank professor Daniel Kirschen, Dr. Hrvoje Pandzic, Ting Qiu, Yishen Wang, and Dr. Mengran Xue for fruitful discussions and for making available the RTS system data, including wind turbine profiles and placement in the RTS-96 system.

References

[1] "Grid 2030 - a national vision for electricity's second 100 years," tech. rep., Federal Energy Regulatory Commission, July 2003.

[2] J. B. Rawlings, "Tutorial overview of model predictive control," *IEEE Control Systems Magazine*, vol. 20, pp. 38–52, Jun 2000.

[3] M. Larsson, D. J. Hill, and G. Olsson, "Emergency voltage control using search and predictive control," *Electrical Power and Energy Systems*, vol. 24, pp. 121–130, Feb 2002.

[4] M. Zima, P. Korba, and G. Andersson, "Power systems voltage emergency control approach using trajectory sensitivities," *IEEE Conference on Control Applications*, vol. 1, pp. 189 – 194, 2003.

[5] I. A. Hiskens and B. Gong, "MPC-based load shedding for voltage stability enhancement," *IEEE Conference on Decision and Control*, Dec 2005.

[6] B. Otomega, A. Marinakis, M. Glavic, and T. Van Cutsem, "Emergency alleviation of thermal overloads using model predictive control," *PowerTech*, pp. 201–206, July 2007.

[7] J. Carneiro and L. Ferrarini, "Preventing thermal overloads in transmission circuits via model predictive control," *IEEE Transactions on Control Systems Technology*, vol. 18, no. 6, pp. 1406 – 1412, 2010.

[8] M. Almassalkhi and I. A. Hiskens, "Cascade mitigation in energy hub networks," *IEEE Conference on Decision and Control*, Dec 2011.

[9] M. Almassalkhi and I. A. Hiskens, "Impact of energy storage on cascade mitigation in multi-energy systems," *IEEE PES General Meeting*, July 2012.

[10] M. Almassalkhi, *Optimization and Model-predictive Control for Overload Mitigation in Resilient Power Systems*. PhD thesis, University of Michigan, 2013.

[11] A. Wood and B. Wollenberg, *Power Generation, Operation, and Control*. Wiley-Interscience, second ed., 1996.

[12] A. L. Motto, F. D. Galiana, A. J. Conejo, and J. M. Arroyo, "Network-constrained multiperiod auction for a pool-based electricity market," *IEEE Transactions on Power Systems*, vol. 17, pp. 646–653, Aug 2002.

[13] R. Palma-Benhke, A. Philpott, A. Jofré, and M. Cortés-Carmona, "Modelling network constrained economic dispatch problems," *Optim Eng*, pp. 1–14, Oct 2012.

[14] M. Almassalkhi and I. A. Hiskens, "Optimization framework for the analysis of large-scale networks of energy hubs," *Power Systems Computation Conference*, Aug 2011.

[15] P. Kundur, N. J. Balu, and M. G. Lauby, *Power System Stability and Control*. McGraw-Hill Education, first ed., 1994.

[16] IEEE Standard 738, *IEEE Standard for Calculating the Current-Temperature of Bare Overhead Conductors*, 2007.

[17] A. Monticelli, *State Estimation in Electric Power Systems: A Generalized Approach*. Springer, 1999.

[18] J. Lee, *A first course in combinatorial optimization*, vol. 36. Cambridge University Press, 2004.

[19] C. Grigg, P. Wong, P. Albrecht, R. Allan, M. Bhavaraju, R. Billinton, Q. Chen, C. Fong, S. Haddad, S. Kuruganty, W. Li, R. Mukerji, D. Patton, N. Rau, D. Reppen, A. Schneider, M. Shahidehpour, and C. Singh, "The IEEE reliability test system," *IEEE Transactions on Power Systems*, vol. 14, no. 3, pp. 1010 – 1020, 1999.

[20] Operations Support Division, "Manual on transmission operations," tech. rep., PJM, Dec 2012.

[21] H. Chavez and R. Baldick, "Inertia and governor ramp rate constrained economic dispatch to assess primary frequency response adequacy," *International Conference on Renewable Energies and Power Quality*, pp. 1–6, Mar 2012.

[22] T. J. Overbye, X. Cheng, and Y. Sun, "A comparison of the AC and DC power flow models for LMP calculations," *Hawaii International Conference on System Sciences*, pp. 1–9, Jan 2004.

[23] S. Talukdar, D. Jia, P. Hines, and B. H. Krogh, "Distributed model predictive control for the mitigation of cascading failures," *IEEE Conference on Decision and Control*, pp. 4440 – 4445, 2005.

[24] G. Hug-Glanzmann and G. Andersson, "Decentralized optimal power flow control for overlapping areas in power systems," *IEEE Transactions on Power Systems*, vol. 24, pp. 327 – 336, Feb 2009.